Wild-type Measles Virus with the Hemagglutinin Protein of the Edmonston Vaccine Strain Retains Wild-type Tropism in Macaques

Kaoru Takeuchi,[1]* Noriyo Nagata,[2] Sei-ich Kato,[1] Yasushi Ami,[3] Yuriko Suzaki,[3] Tadaki Suzuki,[2] Yuko Sato,[4] Yasuko Tsunetsugu-Yokota,[5] Kazuyasu Mori,[6] Nguyen Van Nguyen,[1] Hideki Kimura[1] and Kyosuke Nagata[1]

Department of Infection Biology, Division of Biomedical Science, Faculty of Medicine, University of Tsukuba, Tsukuba 305-8575[1]; Department of Pathology,[2] and Division of Animal Experiments,[3] National Institute of Infectious Diseases, Tokyo 208-0011; Department of Pathology,[4] Department of Immunology,[5] and AIDS Research Center,[6] National Institute of Infectious Diseases, Tokyo 162-8640, Japan

Abstract: 243 words; Main text: 3786 words

Running title: MEASLES VIRUS H PROTEIN AND TROPISM

*Corresponding address:

Kaoru Takeuchi

Department of Infection Biology, Division of Biomedical Science, Faculty of Medicine, University of Tsukuba, 1-1-1 Tennodai, Tsukuba, Ibaraki 305-8575, Japan

Phone: +81-29-853-3472 Fax: +81-29-853-3472

E-mail: ktakeuch@md.tsukuba.ac.jp

ABSTRACT

A major difference between vaccine and wild-type strains of measles virus (MV) in vitro is the wider cell specificity of vaccine strains, resulting from the receptor usage of the hemagglutinin (H) protein. Wild-type H proteins recognize the signaling lymphocyte activation molecule (SLAM; CD150), which is expressed on certain cells of the immune system, whereas vaccine H proteins recognize CD46, which is ubiquitously expressed on all nucleated human and monkey cells, in addition to SLAM. To examine the effect of the H protein on tropism and attenuation of MV, we generated enhanced green fluorescent protein (EGFP)-expressing recombinant wild-type MV strains bearing the Edmonston vaccine H protein (MV-EdH) and compared them to EGFP-expressing wild-type MV strains. In vitro, MV-EdH replicated in SLAM(+) as well as CD46(+) cells, including primary cell cultures from cynomolgus monkey tissues, whereas the wild-type MV replicated in only SLAM(+) cells. However, in macaques, both wild-type MV and MV-EdH strains infected lymphoid and respiratory organs, and wide spread infection of MV-EdH was not observed. Flow cytometric analysis indicated that SLAM(+) lymphocyte cells were infected preferentially with both strains. Interestingly, EGFP expression of MV-EdH in tissues and lymphocytes was significantly weaker than that of the wild-type MV. Taken together, these results indicate that the CD46-binding activity of the vaccine H protein is important for determining the cell specificity of MV in vitro but not the tropism in vivo. They also suggest that the vaccine H protein attenuates the MV growth in vivo.

INTRODUCTION

Measles remains a major cause of childhood morbidity and mortality worldwide especially in developing countries in spite of significant progress in global measles control programs. Measles virus (MV), belonging to the genus *Morbillivirus* of the family Paramyxoviridae, is an enveloped virus with a non-segmented negative-strand RNA genome (11). The MV genome encodes 6 structural proteins: the nucleocapsid (N), phospho (P), matrix (M), fusion (F), hemagglutinin (H), and large (L) proteins. Two envelope glycoproteins, the F and H proteins, initiate infection of the target cells via binding of the H protein to its cellular receptors. Therefore, the H protein is of primarily importance for determining the cell specificity of MV (22).

The Edmonston strain of MV was isolated in 1954 by using a primary culture of human kidney cells (7). The Edmonston strain was subsequently adapted in a variety of cells, including chicken embryo fibroblasts to enable the production of attenuated live vaccines, which are currently used worldwide (27). These live, attenuated MV strains are safe and induce strong cellular and humoral immune responses against MV. The Edmonston vaccine strain is no longer pathogenic in monkey models (2, 7, 37, 39). In contrast, wild-type MV strains isolated and passaged in B95a cells induce clinical signs resembling those of human measles in experimentally infected cynomolgus and rhesus monkeys (15, 16).

A major difference between vaccine and MV wild-type strains in vitro is their cell specificity. Vaccine strains of MV grow efficiently in many human and primate cell lines, whereas wild-type strains of MV grow only in limited lymphoid cell lines. This difference is attributed mainly to the receptor usage of MV strains. The H proteins of

67 wild-type strains recognize the signaling lymphocyte activation molecule (SLAM; also
68 called CD150), which is expressed in certain immune system cells (36), and recently
69 identified nectin-4 (also called PVRL4), which is expressed in epithelial cells in
70 trachea, skin, lung, prostate and stomach as a cellular receptor (20, 23). However, the
71 H proteins of MV vaccine strain recognize CD46 (6, 21) in addition to SLAM and
72 nectin-4 as cellular receptors. Since CD46 is expressed in all human and monkey
73 nucleated cells, MV vaccine strains can grow in many human and primate cell lines.
74 Indeed, when the H protein of a wild-type strain of MV was exchanged with that of an
75 MV vaccine strain, the resulting recombinant wild-type MV strain grew in many
76 human and monkey cell lines (12, 28, 35).

77 Although the receptor specificity of the H proteins of MV strains has been studied
78 extensively, very little is known about the effect of the H protein on the in vivo tropism
79 and attenuation of MV. Given the H proteins of MV vaccine strains can use CD46 in
80 addition to SLAM and nectin-4 as cellular receptors, recombinant MV strains bearing
81 the H protein of MV vaccine strains may have an expanded in vivo tropism.

82 In this study, we generated enhanced green fluorescent protein (EGFP)-expressing
83 recombinant wild-type strains of MV bearing the H protein of the Edmonston MV
84 vaccine strain by using our reverse genetics system (32) and compared the cell
85 specificity in vitro and tropism in vivo with those of EGFP-expressing MV wild-type
86 strains. We found that the H protein of the Edmonston vaccine strain of MV alters the
87 cell specificity of the MV wild-type strain in vitro but does not alter the tropism of the
88 MV wild-type strain in vivo. Furthermore, the H protein of the Edmonston vaccine

89 strain attenuates the MV growth in macaques.

90

91 ## MATERIALS AND METHODS

92 **Cells and viruses**

93 B95a cells (an adherent marmoset B-cell line transformed with Epstein-Barr virus)
94 (15) were maintained in Dulbecco's modified essential medium (DMEM)
95 supplemented with 10% fetal bovine serum (FBS). Chinese hamster ovary (CHO)
96 cells constitutively expressing human SLAM (CHO/hSLAM) (29) were maintained in
97 Rosewell Park Memorial Institute (RPMI) 1640 medium supplemented with 10% FBS
98 and 500 μg of G418 per ml. Primary cynomolgus monkey astroglial cells were
99 obtained from Nobuyuki Kimura (National Institute of Biomedical Innovation,
100 Tsukuba, Japan). IC323-EGFP was obtained from Yusuke Yanagi (Kyushu University,
101 Fukuoka, Japan) (12). Vaccinia virus vTF7-3 encoding T7 RNA polymerase was
102 obtained from Bernard Moss (National Institute of Health, Bethesda, MD) (9).

103

104 **Preparation of primary cynomolgus monkey kidney cells**

105 The kidneys of a cynomolgus monkey were removed, sliced into small pieces, and
106 digested with 0.3% trypsin in Hanks' balanced salt solution (HBBS) at 37°C with
107 continuous stirring for an appropriate period. The dispersed cells were collected and
108 washed twice with HBBS. The cells were suspended in DMEM supplemented with
109 10% FCS, seeded on a plate, and incubated at 37°C. Cells that grew as a monolaye r
110 culture were passaged, and the cells at passages 3 to 5 were used in the experiments.

111

112 **Construction of full-length cDNAs and reverse genetics**

113 Plasmid p(+)MV323, carrying the full-genome cDNA of the IC-B strain has been
114 described previously (15, 32, 33). Plasmid p(+)MV017, carrying the full-genome
115 cDNA of the IC-B strain containing the H gene of the Edmonston B strain (Z66517),
116 has been described previously (35). To exchange the H gene of p(+)MV323-EGFP
117 with that of the Ed strain, a PacI-SpeI fragment containing the H gene was excised
118 from p(+)MV323-EGFP and replaced with the corresponding fragment from
119 p(+)MV017 resulting in p(+)MV017-EGFP. To introduce the EGFP gene between
120 the F and H genes of p(+)MV323 and p(+)MV017, the open reading frame of an
121 enhanced green fluorescent protein (EGFP) gene was first amplified from pEGFP-N1
122 (Clontech, Mountain View, CA) by using the primers
123 5'-ATCAGGGACAAGAGCAGGATTAGGGATATCCGAGATGGTGAGCAAGGGC
124 GAGGA -3' and
125 5'-GATGTTGTTCTGGTCCTCGGCCTCTCGCACTTACTTGTACAGCTCGTCCA-
126 3' and then using the primers
127 5'-GCGTTAATTAAAACTTAGGATTCAAGATCCTATTATCAGGGACAAGAGCA
128 GGAT-3' and
129 5'-GCGTTAATTAACAATGATGGAGGGTAGGCGGATGTTGTTCTGGTCCTCGG-
130 3' to introduce a PacI recognition site (underlined). After digestion with PacI, the
131 EGFP fragment was inserted into the PacI site in p(+)MV323 and p(+)MV017,
132 resulting in p(+)MV323-EGFP(F/H) and p(+)MV017-EGFP(F/H), respectively.

133 Recombinant MV strains, EdH-EGFP, IC323-EGFP$_2$ and EdH-EGFP$_2$, were generated
134 from p(+)MV017-EGFP, p(+)MV323-EGFP(F/H) and p(+)MV017-EGFP(F/H)
135 plasmids, respectively, by using CHO/hSLAM cells and a vaccinia virus vTF7-3 as
136 reported previously (29). IC323-EGFP, EdH-EGFP, IC323-EGFP$_2$, and EdH-EGFP$_2$
137 were propagated in B95a cells, and virus stocks at 3-4 passages in B95a cells were
138 used for experiments. The amino acid sequence of the F protein of the IC-B strains
139 (NC_001498/AB016162) is identical to that of the Edmonston-B strain (Z66517).
140
141 **Infection of cynomolgus monkeys with recombinant MVs**
142 Cynomolgus monkeys were inoculated intranasally with 10^5 times the 50% tissue
143 culture infective dose ($TCID_{50}$) of IC323-EGFP$_2$ or EdH-EGFP$_2$ by using a nasal spray
144 (Keytron, Chiba, Japan). Three animals (#4848, #4849, and #4850) were juvenile (1
145 year old), and 6 animals (#5056, #5057, #5058, #5062, #5068, and #5069) were of 4-5
146 years old. All animals were seronegative for MV. Peripheral blood mononuclear
147 cells (PBMCs) were isolated using a Percoll gradient (Amersham, Piscataway, NJ)
148 diluted with 1.5 M NaCl solution to 1.07 g/ml. MV-infected cells in PBMCs, spleen
149 and cervical lymph nodes were counted as previously reported (32). All animal
150 experiments were performed in compliance with the guidelines of National Institute of
151 Infectious Disease (Tokyo, Japan).
152
153 **Macroscopic detection of EGFP fluorescence**
154 EGFP fluorescence in the tissues and organs of cynomolgus monkeys was observed

using a VB-G25 fluorescence microscope equipped with a VB-7000/7010 charge-coupled device (CCD) detection system (Keyence, Osaka, Japan). For the respective excitation and the detection of fluorescence, 470/40 nm and 510 nm band-pass filters were used.

Histopathological and immunohistochemical analysis

Animals were anesthetized, and tissues from lung, bronchi, heart, liver, kidney, skin, spleen, mesenteric lymph node, cervical lymph node, thymus, salivary gland, tonsil, stomach, pancreas, and jejunum were fixed with 10% phosphate-buffered formalin. Fixed tissues were embedded in paraffin, sectioned, and stained with hematoxylin and eosin. Immunohistochemical detection of the N protein of MV was performed on paraffin-embedded sections as described previously (34).

Double immunofluorescence staining

Paraffin-embedded lungs were used for staining the N protein of MV and cytokeratin. The sections were subjected to a double immunofluorescence staining method employing a rabbit antiserum against the N protein and the cytokeratin monoclonal mouse antibody (clone MAB1611, Chemicon, CA). Briefly, after deparaffinization with xylene, the sections were re-hydrated in ethanol and immersed in phosphate buffered saline (PBS). Antigens were retrieved by hydrolytic autoclaving for 15 min at 121°C in the retrieval solution at pH 9.0 (Nichirei, Tokyo, Japan). After cooling, normal goat serum was used to block background staining.

177 The sections were incubated with the anti-cytokeratin antibody for 30 min at 37°C.
178 After 3 washes in PBS, the sections were incubated with an antiserum against MV N
179 protein for 30 min at 37°C. Antigen-binding sites were detected by goat anti-rabbit
180 Alexa Fluor 488 (Molecular Probes, Eugene, OR) or goat anti-mouse Alexa Fluor 546
181 (Molecular Probes) for 30 min at 37°C. The sections were mounted with SlowFade
182 Gold antifade reagent with DAPI (Molecular Probes), and the images were captured
183 using a fluorescence microscope (IX71; Olympus, Tokyo, Japan) equipped with a
184 Hamamatsu high-resolution digital B/W CCD camera (ORCA2; Hamamatsu Photonics,
185 Hamamatsu, Japan).
186
187 **Flow-cytometric analysis**
188 PBMCs were stained with the following monoclonal antibodies cross-reactive with
189 macaque cells: CD150-phycoerythrin (PE) clone A12 (BD Pharmingen, San Diego,
190 CA), CD3-APC clone SP34-2 (BD Pharmingen) and CD20-PE/Cy7 clone 2H7
191 (BioLegend, San Diego, CA). The cells were fixed with 1% paraformaldehyde and
192 MV-infected cells were detected by the expression of EGFP in the fluorescein
193 isothiocyanate channel. The flow cytometric acquisition of approximately
194 200,000-500,000 events from each sample was performed on FACSCalibur.
195
196 **Amplification of MV genomic RNA by real-time reverse transcription polymerase**
197 **chain reaction (RT-PCR)**
198 Total RNA was isolated from tissues by using the RNAlater and RNeasy kit

(QIAGEN, Hilden, Germany) according to the manufacturer's protocol, reverse transcribed and PCR amplified with a Thermal Cycler Dice TP800 (Takara, Tokyo, Japan) by using FastStart SYBR Green Master (Roche). For amplification of the MV genome sequence, MV-P1 primer 5'-AGATGCTGACTCTATCATGG-3' (positions 2,178-2,197) was used for RT, and then MV-P1 primer and MV-P2 primer 5'-TCGAGCACATTGGGTTGCAC-3' (position 2,574-2,555) were used for PCR. For amplification of the 18S RNA segment, the 18S sense primer TCAAGAACGAAAGTCGGAGG and 18S antisense primer GGACATCTAAGGGCATCACA (25) were used. In a separate experiment, we amplified DNA from a known amount of p(+)MV323-EGFP plasmid containing the target region under the same reaction conditions, and the results for the real-time RT-PCR were expressed as genome RNA equivalent to p(+)MV323-EGFP.

Cytokine assay

Cytokine levels in the plasma were measured with a Luminex 200 (Luminex, Austin, TX) by using a Milliplex Non-Human Primate Cytokine/Chemokine kit (Millipore, Billerica, MA) according to the manufacturer's instruction. The assay sensitivities were as follows; IL-12/23 (p40), 1.11 pg/ml; IFN-γ, 0.30 pg/ml; IL-2, 0.73 pg/ml; IL-4, 1.25 pg/ml; IL-5, 0.26 pg/ml; IL-17, 0.13 pg/ml; IL-6, 0.40 pg/ml; TNF-α, 0.86 pg/ml; IL-1β, 0.16 pg/ml; and MCP-1, 0.91 pg/ml.

RESULTS

221 **Generation of recombinant MV strains expressing EGFP**

222 To compare cell specificity in vitro of wild-type MV and wild-type MV bearing the
223 H protein of the Edmonston vaccine strain, we generated EdH-EGFP from wild-type
224 IC323-EGFP (12). IC323-EGFP and EdH-EGFP (Fig. 1A) have the EGFP gene
225 preceding the N gene and induce a strong EGFP fluorescence in infected monolayer
226 cells. For in vivo infection, we generated IC323-EGFP$_2$ and EdH-EGFP$_2$ (Fig. 1A)
227 having the EGFP gene between the F and H genes, because a previous report using
228 canine distemper virus (CDV) indicated that a CDV strain having the EGFP gene
229 preceding the N gene reduced the overall CDV gene expression and was less virulent
230 (38). IC323-EGFP$_2$ and EdH-EGFP$_2$ induced very weak EGFP fluorescence in
231 infected monolayer cells (data not shown) because of the polar effect of paramyxovirus
232 transcription (17).
233
234 **Infection of primary cell culture with recombinant MV strains**

235 We first examined the cell specificity of IC323-EGFP and EdH-EGFP in vitro. In
236 B95a cells, both IC323-EGFP and EdH-EGFP induced large syncytia and strong EGFP
237 expression, whereas in Vero cells, only EdH-EGFP induced syncytia and strong EGFP
238 expression (Fig. 1B), consistent with our previous observation (35). Notably,
239 EdH-EGFP induced large syncytia and strong EGFP expression in primary kidney and
240 primary astroglial cells derived from cynomolgus monkey tissues (Fig. 1B). Thus,
241 the H protein of the Edmonston vaccine strain of MV can expand the in vitro cell
242 specificity of the wild-type MV strain in established cell lines as well as in primary cell

243 cultures of cynomolgus monkey tissues.

244

245 **Preliminary infection of cynomolgus monkeys with recombinant MV strains**

246 We next examined the in vivo tropism and growth of IC323-EGFP$_2$ and EdH-EGFP$_2$
247 by using 3 cynomolgus monkeys. Prior to the infection of monkeys with
248 IC323-EGFP$_2$ and EdH-EGFP$_2$, we examined the in vitro cell specificity of both
249 strains by using B95a and Vero cells and confirmed that EdH-EGFP$_2$ had the wider in
250 vitro cell specificity (Fig. 1C). Then, one monkey (#4850) was inoculated with
251 IC323-EGFP$_2$, and two monkeys (#4848 and #4849) were inoculated with EdH-EGFP$_2$.
252 At day 7, viremia was observed in all 3 monkeys (Fig. 2A). Upon necropsy at day 7,
253 nearly the same numbers of MV-infected cells were isolated from the cervical lymph
254 nodes of 3 monkeys (Fig. 2A). EGFP fluorescence was observed in many lymphoid
255 tissues, including the cervical lymph nodes, tongue, tonsils, stomach, and
256 gut-associated lymph nodes in 3 monkeys (Fig. 2B). No significant difference was
257 observed in the distribution and intensity of EGFP fluorescence in the internal organs
258 and tissues among the 3 monkeys, indicating that tropism of EdH-EGFP$_2$ was not
259 expanded in vivo.

260

261 **Growth of recombinant MV strains in cynomolgus monkeys**

262 To assess whether these results can be confirmed, 6 monkeys were infected with
263 IC323-EGFP$_2$ or EdH-EGFP$_2$. Three monkeys (#5058, #5062, and #5069) were
264 inoculated with IC323-EGFP$_2$, and 3 monkeys (#5056, #5057, and #5068) were

265 inoculated with EdH-EGFP$_2$. At day 7, viremia was detected in all 6 monkeys, and
266 the number of infected cells was increased at day 10 in most monkeys (Fig. 3A, left).
267 Upon necropsy at day 10, MV-infected cells were isolated from the cervical lymph
268 nodes and spleens of 6 monkeys (Fig. 3A, right). In monkeys infected with
269 IC323-EGFP$_2$ a large number of the lymphocytes (up to 49%) of cervical lymph nodes
270 were infected, whereas in monkeys infected with EdH-EGFP$_2$ a smaller number (0.040
271 to 0.77%) of the lymphocytes of cervical lymph nodes were infected (Fig. 3A, right).
272 Similarly, in monkeys infected with IC323-EGFP$_2$ a large number of the lymphocytes
273 (up to 8.2%) in the spleen were infected, whereas in monkeys infected with
274 EdH-EGFP$_2$ a smaller number (0.032 to 1.5%) of the lymphocytes in cervical lymph
275 nodes were infected (Fig. 3A, right). In all 6 monkeys infected with either
276 IC323-EGFP$_2$ or EdH-EGFP$_2$, substantial amounts of MV genome RNA were detected
277 in the tonsils, cervical lymph nodes, thymus, spleen, mesenteric lymph nodes, inguinal
278 lymph nodes, bone marrow, and lungs (Fig. 3B). We note that the amount of MV
279 genome RNA of EdH-EGFP$_2$-infected monkeys was significantly lower than that of
280 IC323-EGFP$_2$-infected monkeys especially in lungs.
281
282 **Macroscopic detection of EGFP fluorescence in organs and tissues**
283 In all 6 monkeys infected by IC323-EGFP$_2$ or EdH-EGFP$_2$, EGFP fluorescence was
284 macroscopically detected in many lymphoid organs and tissues including the tongue
285 and tonsils, thymus, trachea and lungs, stomach, and gut-associated lymph nodes, upon
286 necropsy at day 10 (Fig. 4). No difference was observed in the distribution of EGFP

287 fluorescence in the internal organs and tissues between monkeys infected with
288 IC323-EGFP$_2$ or EdH-EGFP$_2$, confirming that tropism of EdH-EGFP$_2$ is not expanded
289 in macaques. However, the intensity of EGFP fluorescence in the internal organs and
290 tissues of EdH-EGFP$_2$-infected monkeys was significantly weaker than that of
291 IC323-EGFP$_2$-infected monkeys.
292
293 **Histopathological and immunohistochemical analysis**
294 To further examine tissue and organ tropism of IC323-EGFP$_2$ and EdH-EGFP$_2$, we
295 performed histopathological and immunohistochemical analyses of fixed specimens.
296 In bronchioles, we histopathologically observed bronchiolitis and giant cells with
297 eosinophilic inclusion bodies in monkeys infected with both IC323-EGFP$_2$ and
298 EdH-EGFP$_2$, and MV N antigen was detected in both sections (Fig. 5A). Tissue
299 sections obtained from the bronchiole area were double-stained with anti-MV N and
300 anti-cytokeratin antibodies, which clearly showed infection of EdH-EGFP$_2$ to the
301 epithelial cells (Fig. 5B) as reported for wild-type MV (3, 20), possibly through
302 nectin-4-mediated pathway (18, 20, 23, 31). Interestingly, the N protein was
303 accumulated under the apical plasma membrane of the infected cells (Fig. 5B),
304 suggesting an intracellular transport mechanism for the N protein to the apical plasma
305 membrane. The MV N antigen was detected in the lymphocytes of the spleen,
306 mesenteric and cervical lymph nodes, thymus, salivary gland, tonsils, stomach, and
307 jejunum (Table 1), as well as in epithelia of the lungs, bronchi, tonsils, and stomach but
308 not in the muscles of the heart and in the epithelia of the liver, kidney, skin, tonsils, and

309 stomach of most monkeys. These data again indicated that tropism of EdH-EGFP$_2$
310 was not expanded in macaques.
311
312 **Flow cytometric analysis**
313 To examine the cell tropism of IC323-EGFP$_2$ and EdH-EGFP$_2$ in lymphocytes,
314 EGFP expression in lymphocytes isolated from PBMCs and mesenteric lymph nodes
315 was analyzed by flow cytometry. 0.90% and 8.59% of B lymphocytes in PBMCs and
316 MLN, respectively, and 0.90% and 3.90% of T lymphocytes in PBMCs and MLN,
317 respectively, were infected with IC323-EGFP$_2$ (Fig. 6). Lymphocytes expressing
318 SLAM were infected with IC323-EGFP$_2$ as previously reported (3). Similarly,
319 0.44-0.53% and 1.06-2.23% of B lymphocytes in PBMCs and MLN, respectively, and
320 0.42-0.68% and 0.70-1.44% of T lymphocytes in PBMCs and MLN, respectively, were
321 infected with EdH-EGFP$_2$ (Fig. 6). Lymphocytes expressing SLAM were also
322 infected with EdH-EGFP$_2$. These results indicated that tropism of EdH-EGFP$_2$ was
323 not expanded in lymphocytes of macaques. Interestingly, the number and intensity of
324 EGFP-expressing cells in lymphocytes of EdH-EGFP$_2$-infected monkeys were
325 significantly lower than that of 323-EGFP$_2$-infected monkeys.
326
327 **Cytokine production of infected monkeys**
328 To investigate whether the differences in growth of IC323-EGFP$_2$ and EdH-EGFP$_2$
329 in monkeys were associated with altered host responses to infection, we measured
330 cytokine and chemokine levels in the plasma of infected monkeys. Cytokines

331 selected for analysis were IL-12, IFN-γ, IL-2, IL-4, IL-5, and IL-17 (Th1/Th2 balance),
332 and the IL-6, TNF-α, IL-1β, and MCP-1 (inflammatory response).

333 With Th1-type cytokines, we found that plasma levels of IL-12 were high for 3
334 (#5056, #5057, and #5062) out of 6 monkeys at day 0, slightly elevated at day 3, and
335 then declined by day 7 (Fig. 7). The plasma levels of IL-12 for other 3 monkeys
336 (#5058, #5068, and #5069) were low throughout the experiment. Irrespective of the
337 plasma levels of IL-12, the plasma levels of IFN-γ were elevated in all 6 monkeys.
338 The increase in plasma levels of IL-2 was marginal by day 10 for 5 monkeys. For
339 inflammatory cytokines, the plasma level of MCP-1 was markedly elevated for all
340 monkeys. IL-4, IL-17, and IL-1β were not detected throughout the experiment.
341 Other cytokines (IL-5, IL-6, and TNF-α) were not consistently detected (data not
342 shown).

343 Taken together, there were no significant differences in the cytokine production
344 profile between the monkeys infected with IC323-EGFP$_2$ or EdH-EGFP$_2$, and similar
345 Th1-type and inflammatory response against acute MV infection have occurred in
346 monkeys infected with IC323-EGFP$_2$ or EdH-EGFP$_2$.

347

348 **DISCUSSION**

349 In this study, we compared the cell specificity and tropism of the wild-type strains of
350 MV bearing the H protein of the Edmonston vaccine strain with the wild-type MV
351 strains. Although EdH-EGFP showed the wider cell specificity in cell lines and
352 primary cell cultures (Fig. 1B), the tissue and organ tropism of EdH-EGFP$_2$ was not

353 altered in all 5 infected macaques (Fig. 2 and 4, and Table 1). Since CD46 is
354 ubiquitously expressed in human and monkey cells, EdH-EGFP$_2$ could infect all cells
355 in macaques. However, widespread infection of EdH-EGFP$_2$ in tissues and organs
356 was not observed. This result is not surprising because it was reported that only the
357 lymph nodes and spleen of monkeys were infected with MV vaccine strains (39).
358 Furthermore, it was recently reported that CD11c-positive myeloid cells, such as
359 alveolar macrophage and dendritic cells in lung of monkeys, were infected with an
360 EGFP-expressing recombinant Edmonston strain of MV via an aerosol route (4).
361 This result is consistent with our findings in that the CD46-using Edmonston vaccine
362 strain does not cause widespread infection in the lungs of monkeys, although there is a
363 possibility that the infection of Edmonston strain in lungs may be restricted due to
364 mutations in the N and P/C/V genes which are most important in combating the innate
365 immune system.

366 One possible explanation for the limited infection of EdH-EGFP$_2$ in macaques is the
367 expression level of CD46. Anderson et al. reported that at low CD46 density,
368 infection with the MV vaccine strain will occurs, but subsequent cell-to-cell fusion
369 does not (1). If the expression levels of CD46 are low in cells in the tissues,
370 EdH-EGFP$_2$ may infect those cells, but subsequent cell-to-cell fusion may not occur.
371 In primary cell cultures, gene expression profiles often change when tissue cells are
372 cultured in vitro. Thus, it is likely that the CD46 expression levels of primary cell
373 cultures are high enough for infection with EdH-EGFP. We are now examining the
374 expression levels of CD46 in cell lines and primary cell cultures and in tissues of

375 cynomolgus monkeys. Another possibility for the limited infection of EdH-EGFP$_2$ in
376 macaque tissues is the inefficient replication of MV due to interferons. Yoshikawa et
377 al. reported that primate kidney cells rapidly lose interferon-inducing activity and
378 permit poliovirus replication when the cells are cultured in vitro (40). MV replication
379 in monkey tissues may be inhibited by interferon, whereas MV replication in primary
380 cell cultures can occur due to the lack of interferon-inducing activity.

381 Flow cytometric analysis showed that lymphocytes expressing SLAM were infected
382 with both IC323-EGFP$_2$ and EdH-EGFP$_2$ (Fig. 6). It is known that stimulated
383 lymphocytes can be efficiently infected with MV and that SLAM is highly expressed
384 in stimulated lymphocytes (11). Thus, the activation status of lymphocytes may be
385 important for infection with MV, and infection of unstimulated lymphocytes with
386 EdH-EGFP$_2$ by the CD46-mediated pathway would not result in efficient MV
387 replication. As a result, lymphocytes expressing SLAM may appear to be equally
388 infected with both strains. Recently, two groups revealed that both SLAM and CD46
389 are required for stable transduction of resting human lymphocytes with lentiviral
390 vectors pseudotyped with the vaccine MV F and H proteins (8, 42). Thus, another
391 possibility is that SLAM-binding in addition to CD46-binding may be required for
392 efficient infection of lymphocytes with EdH-EGFP$_2$. SLAM-binding and subsequent
393 signaling (8, 42) may be important for efficient MV infection.

394 A previous study in which monkeys were infected with pathogenic and Edmonston
395 vaccine strains via an aerosol route showed that only the pathogenic strain caused
396 massive infection in lymphoid tissues (4). We also infected monkeys with

397 IC323-EGFP$_2$ and EdH-EGFP$_2$ via the aerosol route, and we found that both strains
398 caused massive infection in lymphoid tissues (Fig. 3). This result indicated that the
399 Edmonston H protein does not influence the extent of infection in lymphoid tissues.
400 Proteins other than the H protein, possibly viral polymerase proteins (30), may regulate
401 MV replication in lymphoid tissues.

402 Suppression of the production of IL-12 was proposed during measles (10). We
403 found that the initial level of IL-12 was high for 3 monkeys (#5056, 5057, and 5062)
404 but low for 3 monkeys (#5058, 5068, and 5069) (Fig. 7). We do not explain the
405 reason for this difference. However, our results indicated that the IL-12 levels were
406 not significantly induced at early time points during MV infection. This result may
407 be consistent with a previous observation of suppressed serum levels of IL-12 during
408 MV infection in rhesus macaques (13, 26). Interestingly, Th1-type cytokines (IFN-γ
409 and IL-2) were induced in all monkeys irrespective of the IL-12 level. The induction
410 of IFN-γ in plasma at early time points is consistent with that in previous reports of
411 human measles (10, 19, 24, 41). A previous study showed no significant induction of
412 IL-2, IL-12, and IFN-γ in monkeys infected with wild-type MV (5). However, in that
413 experiment the induction of IL-2, IL-12, and IFN-γ was measured by quantitating their
414 mRNA by real-time RT-PCR using RNA extracted from PBMCs. Real-time RT-PCR
415 data may not coincide with the actual amounts of cytokines in plasma.

416 In summary, the current study showed that the H protein of the Edmonston vaccine
417 strain alters the cell specificity of wild-type MV in vitro but not the tropism in
418 macaques. SLAM(+) cells were main target for both IC323-EGFP$_2$ and EdH-EGFP$_2$

in macaques. In addition, it is suggested that the Edmonston vaccine H protein attenuates MV growth in vivo especially in a later stage. It has long been proposed that the vaccine H protein attenuates the virus growth in vivo by several mechanisms (e.g., CD46-mediated signaling in infected cells or down-regulation of CD46 in infected cells and subsequent complement-mediated cell lysis) (14). It will be interesting to examine the type I interferon production and the down-regulation of CD46 in MV-infected cells in monkeys infected with EdH-EGFP$_2$ or MV vaccine strains.

ACKNOWLEDGEMENTS

We thank Y. Yanagi and M. Takeda for providing plasmids and cells; B. Moss for vaccinia virus vTF7-3; N. Kimura for primary monkey astroglial cells; A. Harashima, M. Fujino, Y. Sato, Y. Saito, A. Wakutsu, K. Kato, and T. Nishie for excellent technical support; Y. Yasutomi, K. Terao, A. Yamada, T. Sata, H. Hasegawa and K. Komase for valuable discussion and continuous support. We also thank K. Ho for critical reading and valuable comments. This work was supported in part by a grant-in-aid (No. 21022006 and 23659227) from the Ministry of Education, Culture, Sports, Science and Technology of Japan.

REFERENCES

1. Anderson, B. D., T. Nakamura, S. J. Russell, and K.-W. Peng. 2004. High CD46 receptor density determines preferential killing of tumor cells by oncolytic measles

441 virus. Cancer Res. **64**:4919-4926.

442

443 **2. Auwaerter, P. G., P. A. Rota, W. R. Elkins, R. J. Adams, T. DeLozier, Y. Shi, W.**
444 **J. Bellini, B. R. Murphy, and D. E. Griffin.** 1999. Measles virus infection in rhesus
445 macaques: altered immune responses and comparison of the virulence of six different
446 virus strains. J. Infect. Dis. **180**:950-958.

447

448 **3. de Swart, R. L., M. Ludlow, L. de Witte, Y. Yanagi, G. van Amerongen, S.**
449 **McQuaid, S. Yuksel, T. B. H. Geijtenbeek, W. P. Duprex, and A. D. M. E.**
450 **Osterhaus.** 2007. Predominant infection of CD150+ lymphocytes and dendritic cells
451 during measles virus infection of macaques. PLoS Pathog. **3**: e178.

452

453 **4. de Varies, R. D., K. Lemon, M. Ludlow, S. McQuaid, S. Yuksel, G. van**
454 **Amerongen, L. J. Rennick, B. K. Rima, A. D. M. E. Osterhaus, R. L. de Swart, and**
455 **W. P. Duprex.** 2010. In vitro tropism of attenuated and pathogenic measles virus
456 expressing green fluorescent protein in macaques. J. Virol. **84**:4714-4724.

457

458 **5. Devaux, P., G. Hodge, M. B. McChesney, and R. Cattaneo.** 2008. Attenuation of
459 V- or C-defective measles viruses: infection control by the inflammatory and interferon
460 responses of rhesus monkeys. J. Virol. 82:5359-5367.

461

462 **6. Dorig, R. E., A. Marcil, A. Chopra, and C. D. Richardson.** 1993. The human

463 CD46 molecule is a receptor for measles virus (Edmonston strain). Cell **75**:295-305.
464
465 **7. Enders, J. F., and T. C. Peebles.** 1954. Propagation in tissue cultures of cytopathic
466 agents from patients with measles. Proc. Soc. Exp. Biol. Med. **86**:277-286.
467
468 **8. Frecha, C., C. Levy, C. Costa, D. Negre, F. Amirache, R. Buckland, S. J. Russell,**
469 **F.-L. Cosset, and E. Verhoeyen.** 2011. Measles virus glycoprotein-pseudotyped
470 lentiviral vector-mediated gene transfer into quiescent lymphocytes requires binding to
471 both SLAM and CD46 entry receptors. J. Virol. **85**:5975-5985.
472
473 **9. Fuerst, T. R., E. G. Niles, F. W. Studier, and B. Moss.** 1986. Eukaryotic
474 transient-expression system based on recombinant vaccinia virus that synthesizes
475 bacteriophage T7 RNA polymerase. Proc. Natl. Acad. Sci. U. S. A. **83**:8122-8126.
476
477 **10. Griffin, D. E., B. J. Ward, E. Jauregui, R. T. Johnson, and A. Vaisberg.** 1990.
478 Immune activation during measles: interferon-γ and neopterin in plasma and
479 cerebrospinal fluid in complicated and uncomplicated disease. J. Infect. Dis. **161**:
480 449-453.
481
482 **11. Griffin, D. E.** 2007. Measles virus, p. 1551-1585. *In* D. M. Knipe, P. M. Howley, D.
483 E. Griffin, R. A. Lamb, M. A. Martin, B. Roizman, and S. E. Straus (ed.), Fields
484 virology, 5th ed. Lippincott Williams & Wilkins, Philadelphia, PA.

485

486 **12. Hashimoto, K., N. Ono, H. Tatsuo, H. Minagawa, M. Takeda, K. Takeuchi, and**
487 **Y. Yanagi.** 2002. SLAM (CD150)-independent measles virus entry as revealed by
488 recombinant virus expressing green fluorescent protein. J. Virol. **76**:6743-6749.

489

490 **13. Hoffman, S. J., F. P. Polack, D. A. Hauer, M. Singh, M. A. Billeter, R. J. Adams,**
491 **and D. E. Griffin.** 2003. Vaccination of rhesus macaques with a recombinant measles
492 virus expressing interleukin-12 alters humoral and cellular immune responses. J. Infect.
493 Dis. **188**: 1553-1561.

494

495 **14. Kemper, C, and J. P. Atkinson.** 2009. Measles virus and CD46. Curr. Top.
496 Microbiol. Immunol. **330**:31-57.

497

498 **15. Kobune, F., H. Sakata, and A. Sugiura.** 1990. Marmoset lymphoblastoid cells as a
499 sensitive host for isolation of measles virus. J. Virol. **64**:700-705.

500

501 **16. Kobune, F., H. Takahashi, K. Terao, T. Ohkawa, Y. Ami, Y. Suzaki, N. Nagata,**
502 **H. Sakata, K. Yamanouchi, and C. Kai.** 1996. Nonhuman primate models of measles.
503 Lab. Anim. Sci. **46**:315-320.

504

505 **17. Lamb, R. A., and G. D. Parks.** 2007. *Paramyxoviridae*: the viruses and their
506 replication, p. 1449-1496. *In* D. M. Knipe, P. M. Howley, D. E. Griffin, R. A. Lamb, M.

A. Martin, B. Roizman, and S. E. Straus (ed.), Fields virology, 5th ed. Lippincott Williams & Wilkins, Philadelphia, PA.

18. Leonard, V. H. J., P. L. Sinn, G. Hodge, T. Miest, P. Devaux, N. Oezguen, W. Braun, P. B. McCray Jr., M. B. McChesney, and R. Cattaneo. 2008. Measles virus blind to its epithelial cell receptor remains virulent in rhesus monkeys but cannot cross the airway epithelium and is not shed. J. Clin. Invest. **118**:2448-2458.

19. Moss, W. J., J. J. Ryon, M. Monze, and D. E. Griffin. 2002. Differential regulation of interleukin (IL)-4, IL-5, and IL-10 during measles in Zambian children. J. Infect. Dis. **186**:879-887.

20. Muhlebach, M. D., M. Mateo, P. L. Sinn, S. Prufer, K. M. Uhlig, V. H. J. Leonard, C. K. Navaratnarajah, M. Frenzke, X. X. Wong, B. Sawatsky, S. Ramachandran, P. B. McCray, Jr., K. Cichutek, V. von Messling, M. Lopez, and R. Cattaneo. 2011. Adherens junction protein nectin-4 is the epithelial receptor for measles virus. Nature (in press).

21. Naniche, D., G. Varior-Krishnan, F. Cervoni, T. F. Wild, B. Rossi, C. Rabourdin-Combe, and D. Gerlier. 1993. Human membrane cofactor protein (CD46) acts as a cellular receptor for measles virus. J. Virol. **67**:6025-6032.

22. Navaratnarajah, C, K, V. H. J. Leonard, and R. Cattaneo. 2009. Measles virus glycoprotein complex assembly, receptor attachment, and cell entry. Curr. Top. Microbiol. Immunol. **330**:59-76.

23. Noyce, R. S., D. G. Bondre, M. N. Ha, L.-T. Lin, G. Sisson, M.-S. Tsao, C. D. Richardson. Tumor cell marker PVRL4 (Nectin 4) is an epithelial cell receptor for measles virus. ProS Pahog. 7, e1002240.

24. Ohga, S., C. Miyazaki, K. Okada, K. Akazawa, and K. Ueda. 1992. The inflammatory cytokines in measles: correlation between serum interferon-γ levels and lymphocyte subpopulations. Eur. J. Pediatr. **151**: 492-496.

25. Plumet, S., and D. Gerlier. 2005. Optimized SYBR green real-time PCR assay to quantify the absolute copy number of measles virus RNAs using gene specific primers. J. Virol. Methods **128**:79-87.

26. Polack, F. P., S. J. Hoffman, W. J. Moss, and D. E. Griffin. 2002. Altered synthesis of interleukin-12 and type 1 and type 2 cytokines in rhesus macaques during measles and atypical measles. J. Infect. Dis. **185**:13-19.

27. Rota, J. S., Z. D. Wang, P. A. Rota, and W. J. Bellini. 1994. Comparison of sequences of the H, F, and N coding genes of measles virus vaccine strains. Virus Res.

31:317-330.

28. Tahara, M., M. Takeda, F. Seki, T. Hashiguchi, and Y. Yanagi. 2007. Multiple amino acid substitutions in hemagglutinin are necessary for wild-type measles virus to acquire the ability to use receptor CD46 efficiently. J. Virol. **81**:2564-2572.

29. Takeda, M., S. Ohno, F. Seki, K. Hashimoto, N. Miyajima, K. Takeuchi, and Y. Yanagi. 2005. Efficient rescue of measles virus from cloned cDNA using SLAM-expressing Chinese hamster ovary cells. Virus Res. **108**:161-165.

30. Takeda, M., S. Ohno, M. Tahara, H. Takeuchi, Y. Shirogane, H. Ohmura, T. Nakamura, and Y. Yanagi. 2008. Measles viruses possessing the polymerase protein genes of the Edmonston vaccine strain exhibit attenuated gene expression and growth in cultured cells and SLAM knock-in mice. J. Virol. **82**:11979-11984.

31. Takeda, M., M. Tahara, T. Hashiguchi, T. A. Sato, F. Jinnouchi, S. Ueki, S. Ohno, and Y. Yanagi. 2007. A human lung carcinoma cell line supports efficient measles virus growth and syncytium formation via a SLAM- and CD46-independent mechanism. J. Virol. **81**: 12091-12096.

32. Takeda, M., K. Takeuchi, N. Miyajima, F. Kobune, Y. Ami, N. Nagata, Y. Suzaki, Y. Nagai. and M. Tashiro. 2000. Recovery of pathogenic measles virus from

573 cloned cDNA. J Virol **74**:6643-6647.

574

575 **33. Takeuchi, K., N. Miyajima, F. Kobune, and M. Tashiro.** 2000. Comparative
576 nucleotide sequence analyses of the entire genomes of B95a cell-isolated and Vero
577 cell-isolated measles viruses from the same patient. Virus Genes **20**:253-257.

578

579 **34. Takeuchi, K., M. Takeda, N. Miyajima, Y. Ami, N. Nagata, Y. Suzaki, J.**
580 **Shahnewaz, S. Kadota, and K. Nagata.** 2005. Stringent requirement for the C protein
581 of wild-type measles virus for growth in vitro and in macaques. J. Virol. **79**:7838-7844.

582

583 **35. Takeuchi, K., M. Takeda, N. Miyajima, F. Kobune, K. Tanabayashi, and M.**
584 **Tashiro.** 2002. Recombinant wild-type and Edmonston strain measles viruses bearing
585 heterologous H proteins: role of H protein in cell fusion and host cell specificity. J.
586 Virol. **76**:4891-4900.

587

588 **36. Tatsuo, H., N. Ono, K. Tanaka, and Y. Yanagi.** 2000. SLAM (CDw150) is a
589 cellular receptor for measles virus. Nature **406**:893-897.

590

591 **37. van Binnendijk, R. S., R. W. van der Heijden, G. van Amerongen, F. G.**
592 **UytdeHaag, and A. D. Osterhaus.** 1994. Viral replication and development of specific
593 immunity in macaques after infection with different measles virus strains. J. Infect. Dis.
594 **170**:443-448.

595

596 **38. von Messling, V., D. Milosevic, and R. Cattaneo.** 2004. Tropism illuminated:
597 lymphocyte-based pathways blazed by lethal morbillivirus through the host immune
598 system. Proc. Natl. Acad. Sci. USA **101**: 14216-14221.

599

600 **39. Yamanouchi K., Y. Egashira, N. Uchida, H. Kodama, F. Kobune, M. Hayami,**
601 **A. Fukuda, and A. Shishido.** 1970. Giant cell formation in lymphoid tissue of
602 monkeys inoculated with various strains of measles virus. Jpn. J. Med. Sci. Biol.
603 **23**:131-145.

604

605 **40. Yoshikawa, T., T. Iwasaki, M. Ida-Hosonuma, M. Yoneyama, T. Fujita, H.**
606 **Horie, M. Miyazawa, S. Abe, B, Simizu, and S. Koike.** 2006. Role of the alpha/beta
607 interferon response in the acquisition of susceptibility to poliovirus by kidney cells in
608 culture. J. Virol. **80**: 4313-4325.

609

610 **41. Yu X., Y. Cheng, B. Shi, F. Qian, F. Wang, X. Liu, H. Yang, Q. Xu, T. Qi, L.**
611 **Zha, Z. Yuan, R. Ghildyal.** 2008. Measles virus infection in adults induces production
612 of IL-10 and is associated with increased CD4+CD25+ regulatory T cells. J. Immunol.
613 **181**: 7356-7366.

614

615 **42. Zhou, Q., I. C. Schneider, M. Gallet, S. Kneissl, C. J. Buchholz.** 2011. Resting
616 lymphocyte transduction with measles virus glycoprotein pseudotyped lentiviral vectors

relies on CD46 and SLAM. Virology **413**: 149-152.

FIGURE LEGENDS

FIG. 1. Generation, dissemination, and growth of recombinant measles virus (MV) having the hemagglutinin (H) protein of the Edmonston vaccine strain. (A) Schematic diagram of genomic organization of IC323-EGFP, EdH-EGFP, IC323-EGFP$_2$, and EdH-EGFP$_2$. (B) B95a, Vero, primary cynomolgus monkey kidney (Primary kidney), and primary cynomolgus monkey astroglial (Primary astroglia) cells were infected with IC323-EGFP or EdH-EGFP. The MV-infected cells were visualized with EGFP auto fluorescence at day 2 (B95a), at day 3 (Vero), at day 4 (Primary kidney) and at day 3 (Primary astroglia). (C) Replication kinetics of IC323-EGFP$_2$ and EdH-EGFP$_2$. B95a cells and Vero cells were infected with IC323-EGFP$_2$ (circle) or EdH-EGFP$_2$ (triangle) at an MOI of 0.01 $\times$ tissue culture infective dose (TCID$_{50}$)/cell. Cells and media were harvested at days 0, 1, 2, 3, and 4, and infectivity titers were assessed as TCID$_{50}$ using B95a cells.

FIG. 2. Detection of MV-infected cells in peripheral blood mononuclear cells (PBMCs) and cervical lymph nodes and EGFP expression in the tissues and organs of infected macaques. (A) One monkey (#4850; closed circle) was infected with IC323-EGFP$_2$ and 2 monkeys (#4848 and #4849; open triangle and open square, respectively) were infected with EdH-EGFP$_2$. Single-cell suspensions (10^5/ml) from PBMCs and cervical lymph nodes (CLN) were divided into 2-fold serial dilutions.

639 Then, a 1-ml aliquot of each diluted single-cell suspension was inoculated into
640 subconfluent B95a cells on 24-well cluster plates in duplicate. The number of
641 MV-infected cells per 10^5 single-cell suspensions was then calculated. (B) At day 7,
642 EGFP fluorescence in the tongue and tonsils (a, e, and i), cervical lymph nodes (b, f,
643 and j), stomach (c, g, and k), and gut-associated lymph nodes (d, h, and l), was
644 detected using a fluorescent charge-coupled device (CCD) camera. White arrows
645 indicate the MV-infected regions expressing EGFP.
646
647 **FIG. 3. Detection of MV-infected cells and MV genome RNA.** (A) Three
648 monkeys (#5058, #5062, and #5069) (closed circle, closed triangle, and closed square,
649 respectively) were infected with IC323-EGFP$_2$, and 3 monkeys (#5056, #5057, and
650 #5068; open circle, open triangle, and open square, respectively) were infected with
651 EdH-EGFP$_2$. PBMCs were obtained at days 3, 7, and 10. CLN and spleens were
652 obtained on day 10. Single-cell suspensions (10^5/ml) from PBMCs, CLN and spleen
653 were divided into 2-fold serial dilutions. Then, a 1-ml aliquot of each diluted
654 single-cell suspension was inoculated into subconfluent B95a cells on 24-well cluster
655 plates in duplicate. The number of MV-infected cells per 10^5 single-cell suspensions
656 was then calculated. (B) MV genome RNA was detected by real-time reverse
657 transcription polymerase chain reaction on total RNA isolated from tonsils, CLN,
658 thymus, spleens, mesenteric lymph nodes (MLN), inguinal lymph nodes (IngLN), bone
659 marrow (Bone M), and lungs. Three monkeys (#5058, #5062 and #5069) were
660 infected with IC323-EGFP$_2$, and 3 monkeys (#5056, #5057, and #5068) were infected

661 with EdH-EGFP$_2$. The results for the real-time RT-PCR were expressed as genome
662 RNA equivalent to plasmid p(+)MV323-EGFP.
663
664 **FIG. 4. EGFP expression in tissues of monkeys after experimental infection with**
665 **IC323-EGFP$_2$ and EdH-EGFP$_2$.** At day 10 days, EGFP fluorescence in the tongue
666 and tonsils (a, f, and k), thymus (b, g, and l), trachea and lung (c, h, and m), stomach (d,
667 i, and n), and gut-associated lymph nodes (e, j, and o) of infected monkeys were
668 detected using a fluorescent CCD camera.
669
670 **FIG. 5. Histopathological and immunohistochemical analysis.** (A) Bronchiole
671 sections obtained from monkeys infected with IC323-EGFP$_2$ or EdH-EGFP$_2$ were
672 examined by hematoxylin and eosin staining and immunohistochemistry. Giant cell
673 formation (*) and lymphoid filtrares were seen in the epithelial layer of the bronchiole.
674 MV nucleocapsid (N) antigen (light brown) was detected in the cytoplasm and nucleus
675 in the giant cells and in the cytoplasm of the lymphocytes (arrows) of lymphatic nodule
676 under the epithelial layer by immunohistochemical analysis (IHC). (B) Bronchiole
677 area obtained from monkey infected with EdH-EGFP$_2$ was investigated by double
678 immunofluorescence staining. Tissue sections were stained with antiserum against
679 the MV N antigen and mouse monoclonal antibody against cytokeratin. DAPI was
680 used to identify nuclei. Br, Bronchiole; LN, lymphatic nodule; Bar, A, 50 μm; B, 100
681 μm.
682

683 **FIG. 6. EGFP-positive cells in lymphocyte subpopulations of PBMCs and**
684 **mesenteric lymph nodes from infected monkeys.** (A) Cryopreserved PBMCs and
685 mesenteric lymph nodes (MLN) of monkeys infected with IC323-EGFP$_2$ (#5058) or
686 EdH-EGFP$_2$ (#5057 and #5068) were stained with monoclonal antibodies against CD3,
687 CD20 and CD150 (signaling lymphocyte activation molecule; SLAM), and analyzed in
688 a FACScalibur. Results are shown as dot plots, with SLAM expression on the x-axis
689 and EGFP expression on the y-axis. EGFP expression in CD20$^+$ B-lymphocytes and
690 CD3$^+$ T-lymphocytes are shown. (B) CD46 expression in lymphocytes of PBMCs of
691 monkeys infected with EdH-EGFP$_2$ (#5057 and #5068) was detected with monoclonal
692 antibody against CD46 and isotype control antibody.
693
694 **FIG. 7. Detection of cytokines in the plasma of infected monkeys.** Three
695 monkeys (#5058, #5062, and #5069; closed circle, closed triangle and closed square,
696 respectively) were infected with IC323-EGFP$_2$. Three monkeys (#5056, #5057, and
697 #5068; open circle, open triangle and open square, respectively) were infected with
698 EdH-EGFP$_2$. Plasma was obtained at days 0, 3, 7, and 10. Cytokine levels in the
699 plasma were measured with a Luminex 200 using a Milliplex Non-Human Primate
700 Cytokine/Chemokine kit. The physiological upper concentration ranges detected in
701 human plasma are indicated by dotted lines.

Fig. 1

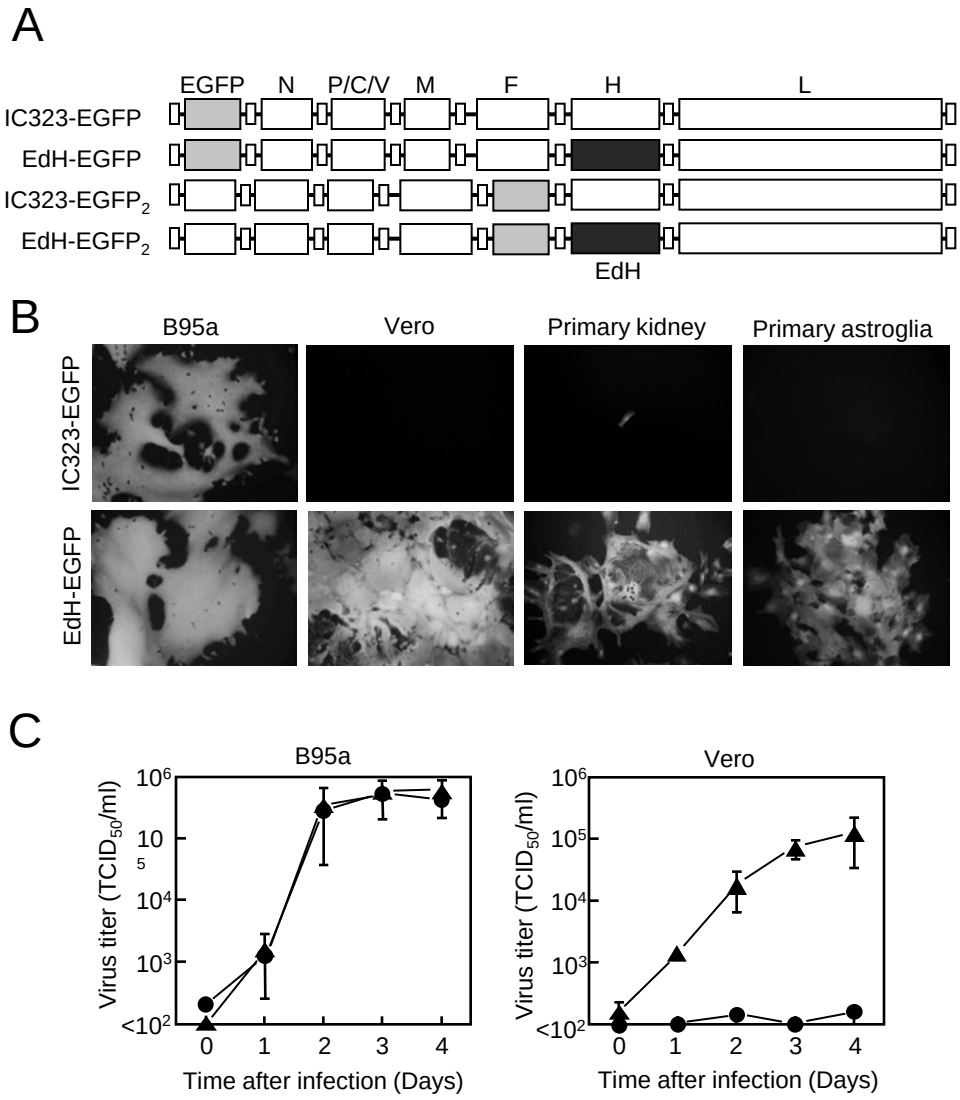
A
EGFP
N
P/C/V
M
F
H
L
IC323-EGFP
EdH-EGFP
IC323-EGFP2
EdH-EGFP2
EdH
B
B95a
Vero
Primary kidney
Primary astroglia
IC323-EGFP
EdH-EGFP
C
B95a
Vero
Virus titer (TCID50/ml)
Time after infection (Days)

Fig.2

A

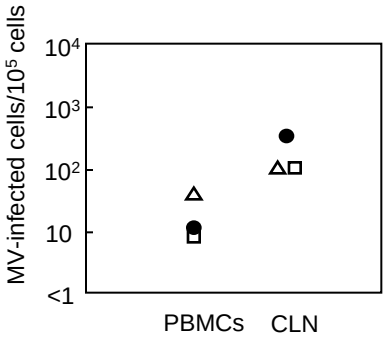
MV-infected cells/10^5 cells
10^4
10^3
10^2
10
<1
PBMCs
CLN

B

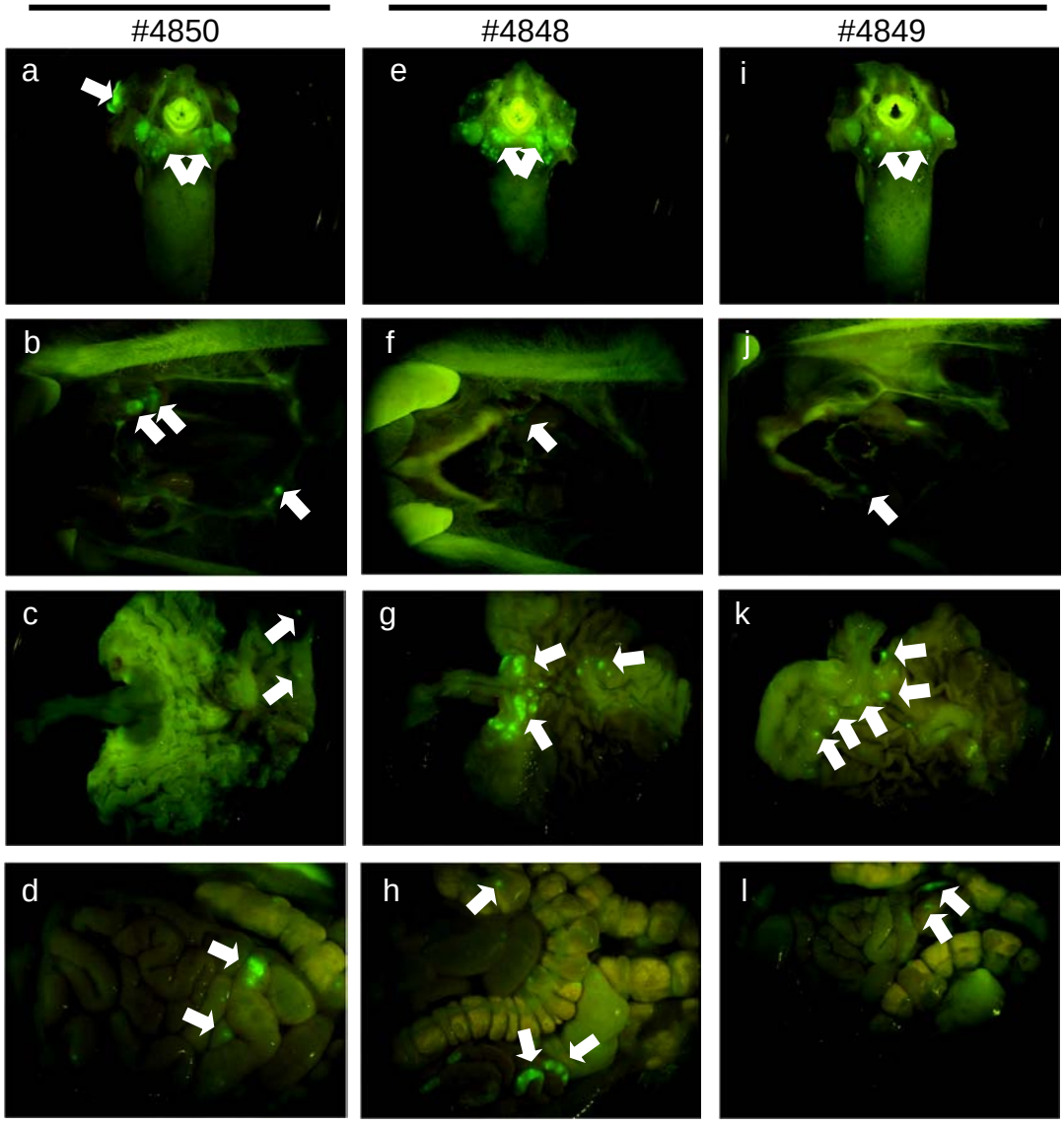
IC323-EGFP2
EdH-EGFP2
#4850
#4848
#4849
a
b
c
d
e
f
g
h
i
j
k
l

Fig.3

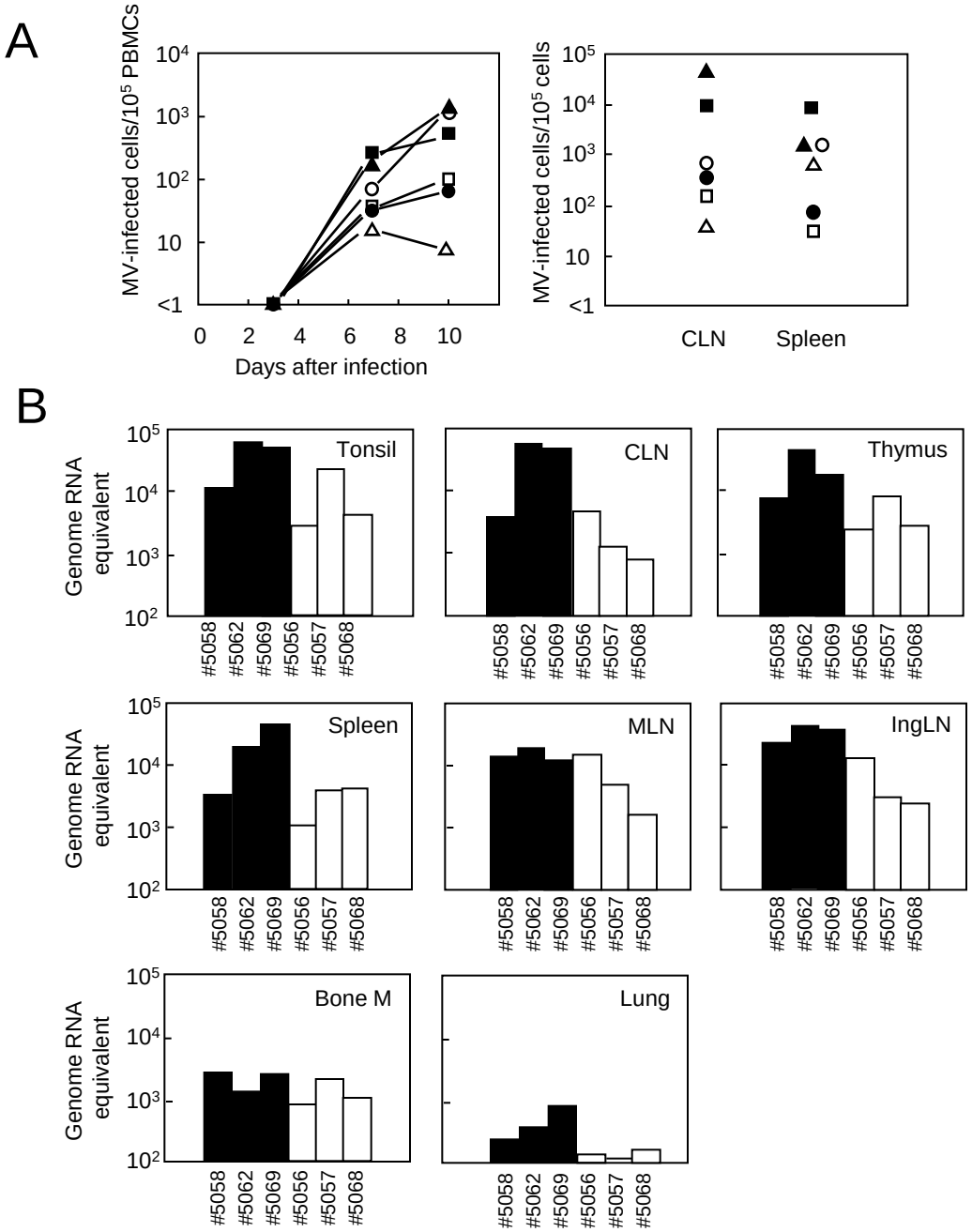
A
MV-infected cells/10^5 PBMCs
10^4
10^3
10^2
10
<1
0 2 4 6 8 10
Days after infection
MV-infected cells/10^5 cells
10^5
10^4
10^3
10^2
10
<1
CLN
Spleen
B
Genome RNA equivalent
Tonsil
CLN
Thymus
Spleen
MLN
IngLN
Bone M
Lung
10^5
10^4
10^3
10^2
#5058 #5062 #5069 #5056 #5057 #5068

Fig.4

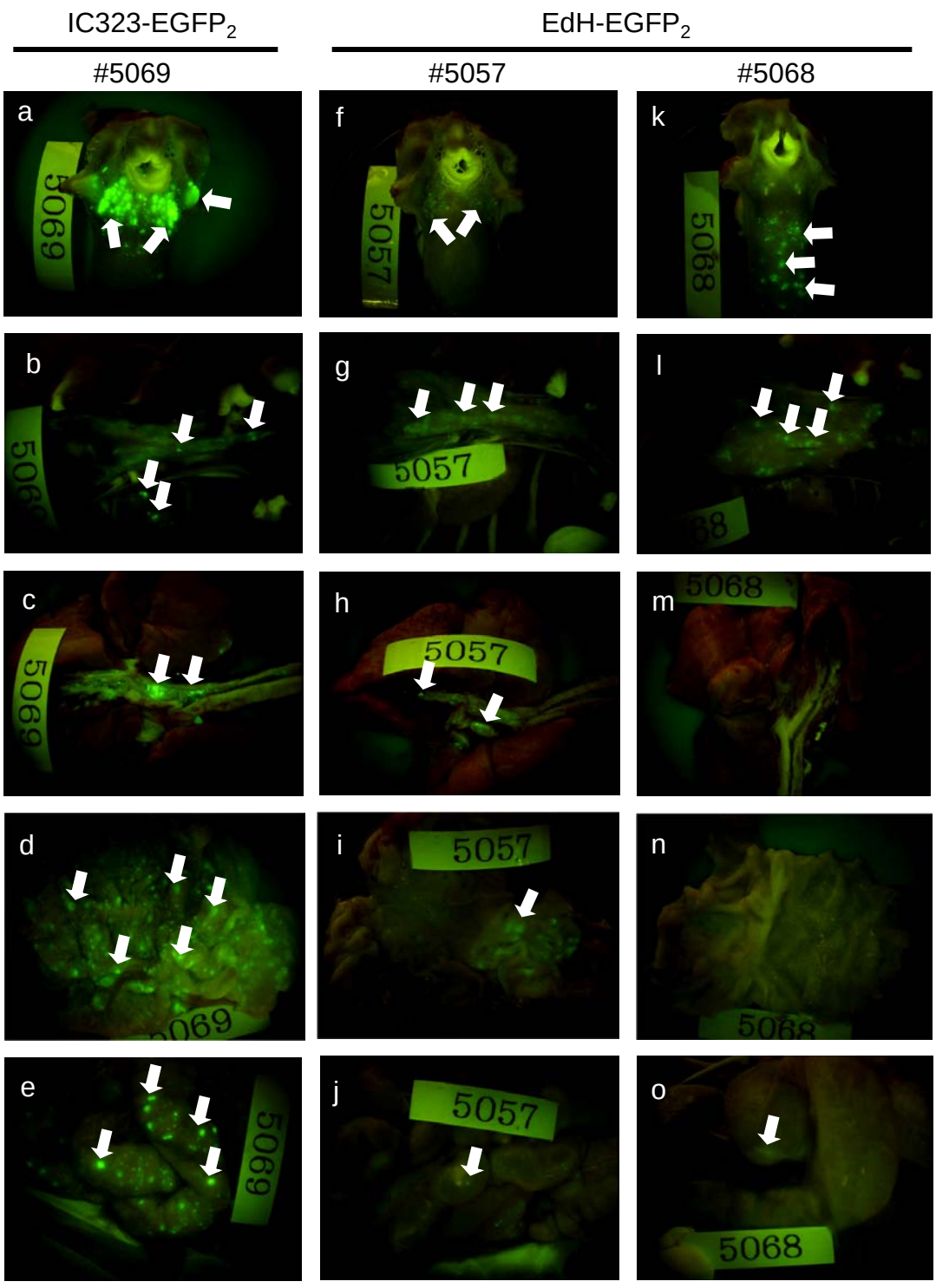
IC323-EGFP2
EdH-EGFP2
#5069
#5057
#5068
a
f
k
b
g
l
c
h
m
d
i
n
e
j
o
5069
5057
5068

Fig.5

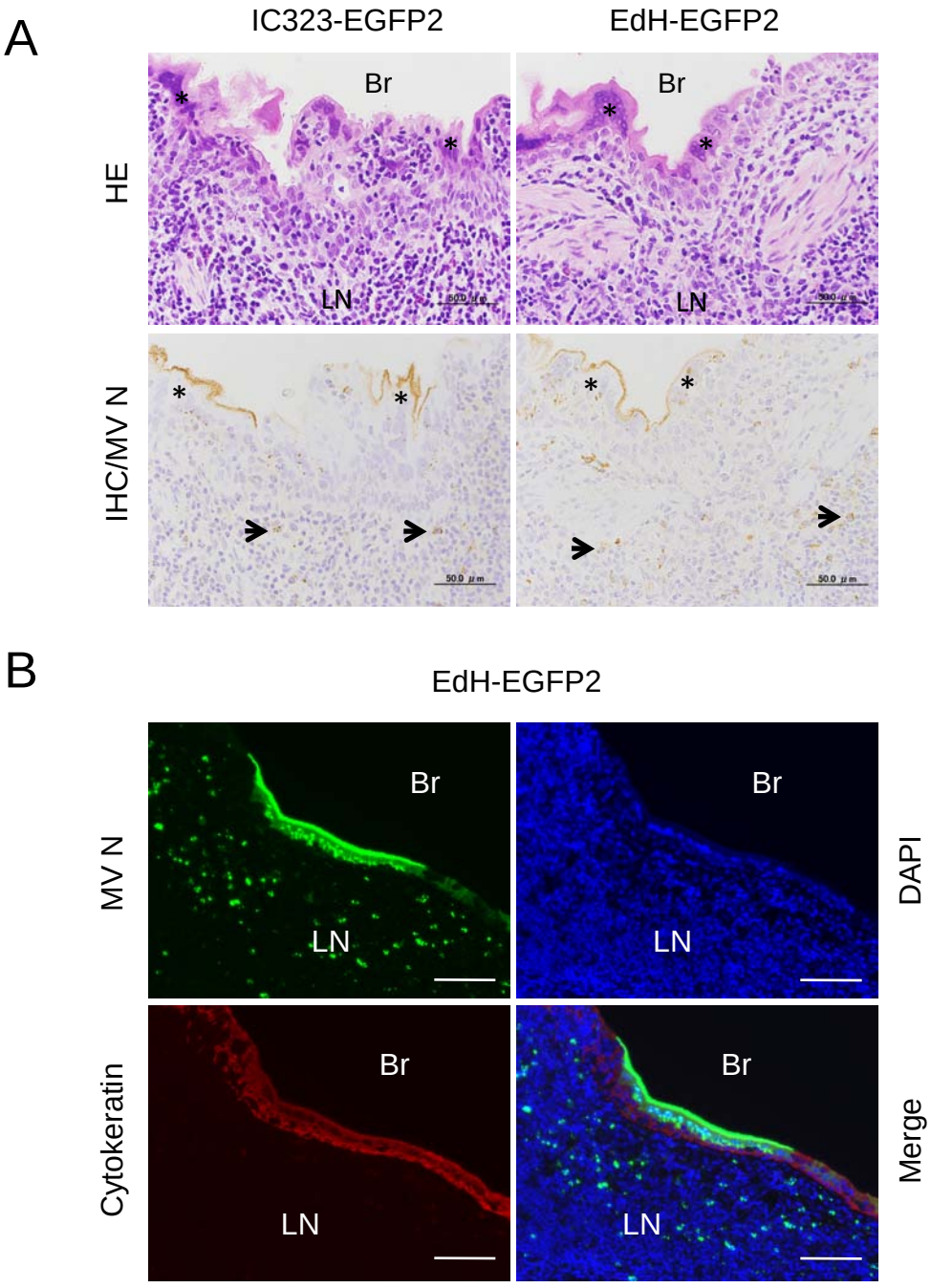
A
IC323-EGFP2
EdH-EGFP2
HE
IHC/MV N
Br
LN
B
EdH-EGFP2
MV N
DAPI
Cytokeratin
Merge

Fig.6

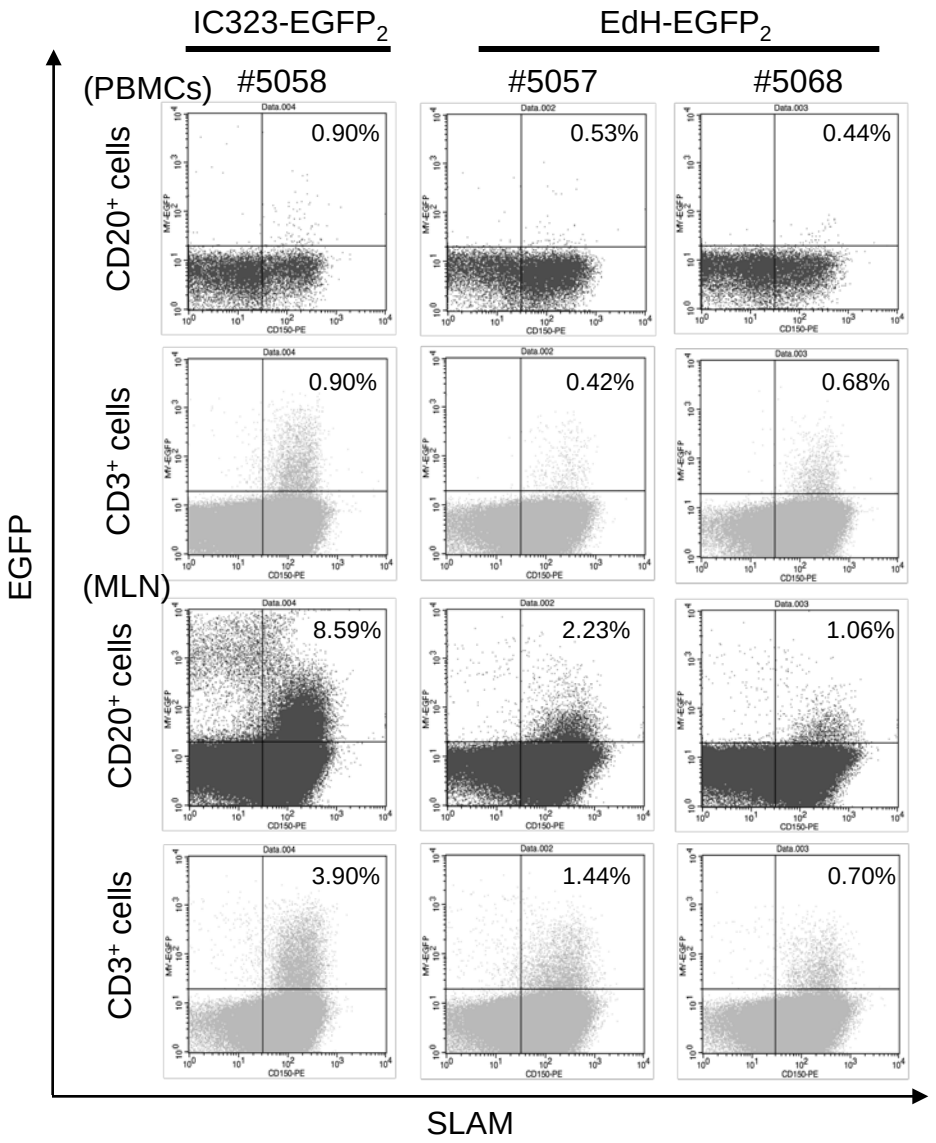
IC323-EGFP2
EdH-EGFP2
(PBMCs)
#5058
#5057
#5068
CD20+ cells
CD3+ cells
(MLN)
CD20+ cells
CD3+ cells
0.90%
0.53%
0.44%
0.90%
0.42%
0.68%
8.59%
2.23%
1.06%
3.90%
1.44%
0.70%
EGFP
SLAM

Fig.7

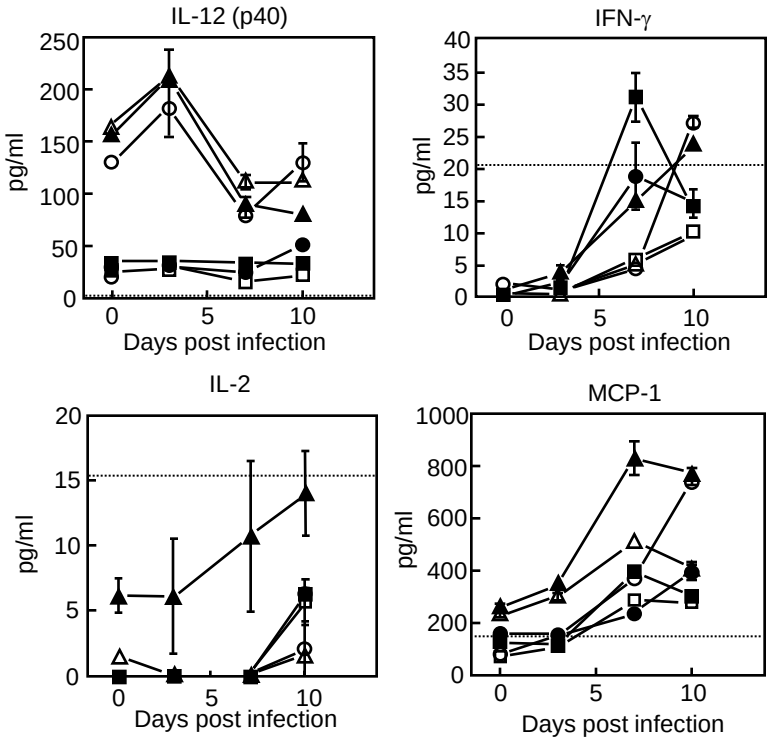
IL-12 (p40)
pg/ml
250
200
150
100
50
0
0
5
10
Days post infection
IFN-γ
pg/ml
40
35
30
25
20
15
10
5
0
0
5
10
Days post infection
IL-2
pg/ml
20
15
10
5
0
0
5
10
Days post infection
MCP-1
pg/ml
1000
800
600
400
200
0
0
5
10
Days post infection